Human Knee Abnormality Detection from Imbalanced sEMG Data

Ankit Vijayvargiya[a,*], Chandra Prakash[b], Rajesh Kumar[a], Sanjeev Bansal[c], João Manuel R. S. Tavares[d]

[a]*Department of Electrical Engineering, Malaviya National Institute of Technology, Jaipur, India*
[b]*Department of Computer Science and Engineering, NIT, Delhi, India*
[c]*Department of Physical Medicine and Rehabilitation, Sawai Man Singh Hospital, Jaipur, India*
[d]*Instituto de Ciência e Inovação em Engenharia Mecânica e Engenharia Industrial, Departamento de Engenharia Mecânica, Faculdade de Engenharia, Universidade do Porto, Porto, Portugal*

Abstract

The classification of imbalanced datasets, especially in medicine, is a major problem in data mining. Such a problem is evident in analyzing normal and abnormal subjects about knee from data collected during walking. In this work, surface electromyography (sEMG) data were collected during walking from the lower limb of 22 individuals (11 with and 11 without knee abnormality). Subjects with a knee abnormality take longer to complete the walking task than healthy subjects. Therefore, the SEMG signal length of unhealthy subjects is longer than that of healthy subjects, resulting in a problem of imbalance in the collected sEMG signal data. Thus, the development of a classification model for such datasets is challenging due to the bias towards the majority class in the data. The collected sEMG signals are challenging due to the contribution of multiple motor units at a time and their dependency on neuromuscular activity, physiological and anatomical properties of the involved muscles. Hence, automated analysis of such sEMG signals is an arduous task. A multi-step classification scheme is proposed in this research to overcome this limitation. The Wavelet Denoising (WD) scheme is used to denoise the collected sEMG signals, followed by the extraction of eleven time-domain features. The oversampling techniques are then used to balance the data under analysis

*Corresponding author
Email addresses: ankitvijayvargiya29@gmail.com (Ankit Vijayvargiya), cse.cprakash@gmail.com (Chandra Prakash), rkumar.ee@mnit.ac.in (Rajesh Kumar), sanjivbansal1899@gmail.com (Sanjeev Bansal), tavares@fe.up.pt (João Manuel R. S. Tavares)

by increasing the training minority class. The competency of the proposed scheme was assessed using various computational classifiers with 10 fold cross-validation. It was found that the oversampling techniques improve the performance of all studied classifiers when applied to the studied imbalanced sEMG data.
Keywords:
Surface Electromyography, Wavelet Denoising, Oversampling Techniques, Imbalanced Data, Machine Learning.

---

1. Introduction

Knee pain is a common complaint that affects the autonomy of individuals of all ages. As per the survey [1], one in every three people have arthritis or joint symptoms in the 18-64 age group due to an injury or underlying condition such as knee osteoarthritis. The knee joint is a synovial joint that acts as a shock absorber and provides stability to the body. The knees join the femur (thigh bone) and come to the tibia (shin bone). The patella (knee cap) and fibula are the other bones that form the knee joint. The bones of the knee are attached to the muscles along with the tendon. The articular cartilage is a thin cartilage between the femur and tibia and provides a smooth movement to these bones [2].

Neuromusculoskeletal disorders such as cerebral palsy and osteoarthritis are other infirmities that reduce the quality of life of people [3, 4]. Clinically, such diseases are diagnosed using X-Ray [5] or Magnetic Resonance Imaging (MRI) techniques [6]. X-ray technique is primary used for gathering and evaluation of the bone status while MRI provides the detailed information of knee structure such as cartilage, ligaments and tendons. MRI is an efficient way for diagnosing but at a higher cost. Knee abnormalities can be diagnosed through wearable sensors such as electromyography (EMG), accelerometer and gyrometer, or by visual sensors such as imaging cameras. A comprehensive review of available gait approach and analysis of applications based on gait data was discussed by chandra prakash and others [7]. EMG sensors allow the recognition of movements in advance [8] while providing faster detection of signal variations [9], and are therefore superior in the investigation of neuromusculoskeletal disorders.

The signal collected by EMG sensors is a biomedical signal that quantifies the electrical activity produced by skeletal muscles. Surface electromyography (sEMG) and intramuscular EMG (iEMG) techniques are popular approaches used to acquire EMG signals [10]. sEMG presents an advantages over iEMG, as the electrodes can be applied without pain or medical monitoring, and additionally the possibility of infection is negligible. Long-term control is often simpler with surface electrodes than using iEMG needles. The placement of the sEMG sensors has a significant influence on the acquired signal and their consequent analysis and recognition by the computational algorithm as confirmed in [11]. sEMG sensors can collect data during daily human activities such as sitting, standing, walking and climbing, which can be used to detect anomalies, actions recognition, etc [12].

sEMG signals are being employed in different applications such as automatic control of lower and upper limb prosthesis or exoskeletons [13], diagnosis of neuromuscular disorders [14] and exercise, fitness monitoring [15]. Khimraj et al. classified six movements of lower limb and compared the results of the computational classifiers [16]. Hudgins et al. proposed a pattern recognition based approach with time-domain features and a multilayer perceptron neural network for the classification of four types of limb motions [17] using sEMG signals. Huang et. al. estimated from sEMG signals the human arm joint torque using a back-propagation neural network (BPNN) and auto encoders [18]. Silva et al. studied the spinal cord injury using the sEMG signal collected during activities of the upper limb [19]. Sudarsan et al. designed and developed an artificial limb controlled by sEMG signals [20]. Tuncer et. al. proposed the ternary pattern and discrete wavelet based feature extraction for hand movement recognition from sEMG signal for amputee people [21]. The Support Vector Machine (SVM) based classification of different upper limb movements performed by five healthy subjects was investigated by Cai et al. [22]. A linear time series based prediction models were proposed by chandra prakash and others. These models can be used for efficient control of robotic assistive devices for lower limb for a smooth movement [23].

In the last decade, researchers have focused on the classification of sEMG sig-nals from the upper limb. The sEMG signals acquired from the lower limb are more challenging as it got influence from overlapping muscles [24, 25]. The classification

of sEMG data from the lower limb has been studied using different signal processing techniques [26, 27]. The human lower limb flexion/extension joint angles were estimated from sEMG signal using a deep belief network by Chen et al. [28]. Bonato et al. investigated the fatigue of quadriceps and hamstring muscles based on sEMG signal [29]. Swaroop et al. used sEMG signal for myopathy and neuropathy classification using a neural network based approach [30]. Kugler et al. used a SVM based solution for the recognition of Parkinson's disease from sEMG data [31]. Morbidoni et al. classified the gait phase while walking from sEMG data with the help of a deep learning based approach [32]. Characterization of walking patterns and using computational techniques are classified into normal and gait pathology [33].

Class imbalance is a challenging issue in medical data. Class imbalance occurs in the case where a varying quantity, i.e. different number, of total samples is present in different data classes. So, if imbalanced data appears in the classification, the result will be swayed toward the majority class [23]. Therefore, for improving the diagnosis success, it is required to balance the data either by increasing the minority class (oversampling) or reducing the majority class (under sampling). Rajesh et al. classified five groups of heartbeat with imbalanced ECG beat using the AdaBoost ensemble classifier [34]. Past studies show that oversampling techniques can overcome the class imbalance problem [35, 36]. Taft et al. applied the Synthetic Minority Oversampling Technique (SMOTE) to enhance the performance of a classification model for the identification of adverse drug events in women admitted for labor and delivery [36].

During walking, the imbalance problem of the acquired sEMG data may occur because of two reasons:

1. The number of abnormal subjects is inferior to the number of healthy subjects;
2. the length of the data collected from abnormal subjects is different from the one obtained from normal subjects.

A person with knee abnormality takes longer to complete the movement task resulting in larger signal length in contrast to a healthy (or control) subject. Hence, the large length of the sEMG signal of the abnormal subject leads to a class imbalance problem. In the present study, two classes with the same number of subjects have been taken;

however, the signal length of each class is different. Figure 1(a) and (b) exhibit the sEMG data acquired from one normal subject and one abnormal subject respectively while performing the same gait task, respectively. It can be observed that the lengths of the acquired sEMG signals have varying lengths.

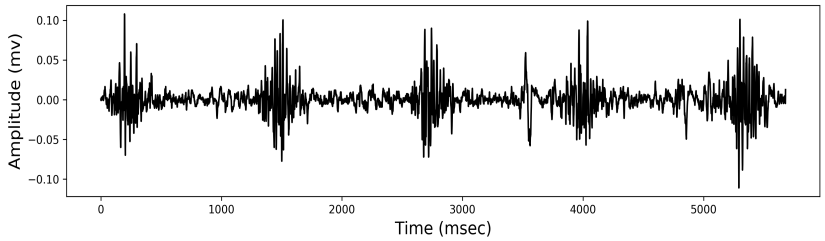

(a)

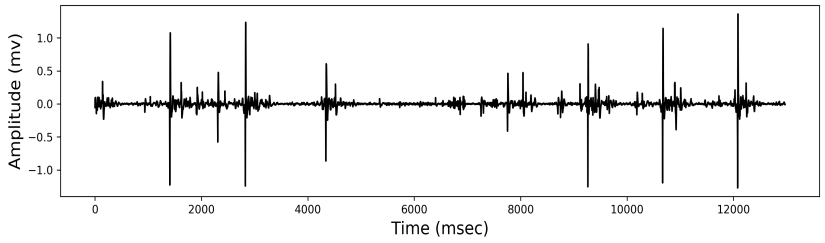

(b)

Figure 1: sEMG signals acquired during gait from: a) a healthy subject and b) an abnormal Knee subject.

As per the author's knowledge, there is no literature/study that resolves the problem of identifying knee abnormality from imbalanced sEMG gait data. Therefore, this paper presents for the first time the problem of identifying a knee abnormality from class imbalanced sEMG data and evaluated the performance parameters of various machine learning classifiers when applied to a balanced and imbalanced sEMG data. The data considered here include 1) original imbalanced data and 2) balanced data that have been obtained through the application of oversampling techniques on the original data. The major contributions of this work are:

1. Identification of knee abnormality from imbalanced sEMG dataset, where sEMG signal length differ between normal and abnormal subjects.
2. Evaluation of metrics (MSE, MAE, SNR and PSNR) for selecting optimal mother wavelet and decomposition level of DWT wavelet;

3. Extraction of eleven discrete wavelet transform (DWT) based features by splitting the sEMG signal into various frequency bands.
4. Evaluating the impact of oversampling techniques on the performance indices of classification models.

This article is organized as follows. A description of the dataset data that has been utilized in the presented work is given in Section II. Section III presents the proposed methodology. Results and their discussion are presented in Sections IV & V, respectively. Under Section VI, conclusions and perspectives of future work have been elaborated.

2. sEMG dataset

The sEMG signal data used in this study has been publicly made available to the UCI machine learning repository by Sanchez et al [37]. The data consist of sEMG signals of the lower limbs of 22 subjects over 18 years of age, where 11 subjects are healthy and 11 subjects have known knee abnormalities. The healthy subjects do not have previous record of knee injury or pain. One abnormal knee subject suffered from sciatic nerve injury, six abnormal subjects had anterior cruciate ligament (ACL) injury and the remaining four suffered from a meniscus injury. The data was collected using a DataLog MWX8 from Biometrics Ltd. and a goniometer when the subjects were performing one of three different tasks: walking, flexion of the leg up and leg extension from sitting position. The sEMG data were recorded for the four muscles: biceps femoris (BF), vastus medialis (VM), rectus femoris (RF) and semitendinosus(ST), with the goniometer attached to the external side of the knee joint. The affected limb of the subject with abnormal knee and the left leg of the healthy subjects were chosen for acquiring the sEMG signal. The data was acquired according to a sampling frequency of 1000 Hz and 14-bit of resolution. The sEMG signals have already been filtered using a band pass filter with a pass band frequency of 20 Hz to 460 Hz. The recorded data does not contain any signal corresponding to the transition states, i.e., standing to sitting, sitting to walking, walking to standing, etc. The data was transferred directly from the MWX8 device to the computer by bluetooth in real-time. Only the sEMG

signals acquired during the walking task were used the experiments performed for this study.

3. Proposed Methodology

This section presents the methodology proposed for the identification of knee abnormality from imbalanced sEMG signal data collected during walking. Figure 2 presents the general flow of the proposed methodology.

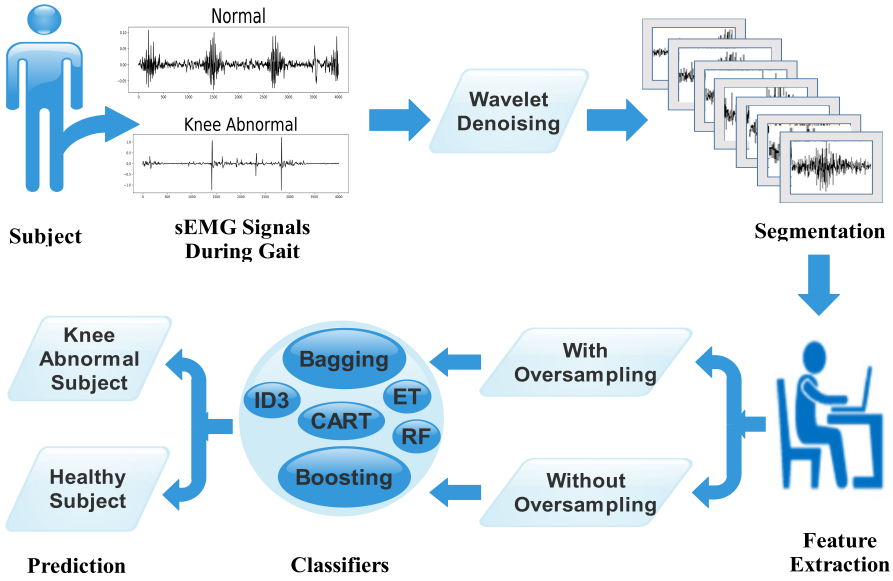

Figure 2: Block diagram of the proposed methodology for abnormality knee detection from sEMG signal collected during walking.

Feature extraction from the collected sEMG signals requires signal pre-processing. The dataset is already preprocessed with band pass filter with a pass band frequency of 20 to 460 Hz. To remove the random noise discrete wavelet denoising technique has been used. The mother wavelet and level of decomposition of the wavelet denoising based on DWT were selected from the mean squared error (MSE), mean absolute error (MAE), signal to noise ratio (SNR) and peak signal to noise ratio (PSNR) values. Thereafter, eleven time-domain features were extracted by the use of an overlapping

windowing technique with a window length of 256 ms and an overlapping of 25% and then the samples of the features were normalized in between 0 (zero) to 1 (one) by the use of Min-max normalization method. Since the data length of healthy and unhealthy subjects are not the same, therefore the number of samples of the extracted features for both conditions, i.e., classes, are also not equal. Hence, in order to balance the samples of the used features, different over-sampling techniques have been used.

The main sections of the proposed methodology presented in Figure2 have been explained in the following subsection:

3.1. Wavelet Denoising

Four types of noises are usually introduced while recording sEMG signals [38]: 1) Ambient noise generated by electromagnetic appliances, 2) Inherent noise result-ing from electronic devices, 3) Motion artifacts produced due to the movement of the sEMG electrodes, and 4) Inherent noise instability due to the firing rate of the involved motor units. Therefore, signal denoising is an essential task that should be performed before using the signals for classification purposes. Conventional filtering techniques like High Pass, Low Pass or Band Pass, can be used to minimize the noise which is not within the range of the active sEMG signal spectrum band. The sEMG signals have been passed through the band pass filter (20 to 460 Hz). Recently, novel methods such as Wavelet Denoising, Independent Component Analysis (ICA) and Empirical Mode Decomposition (EMD), have been successfully used in recent studies to minimize noise from sEMG signals [39, 40, 41].

Over the past few years, the use of Wavelet Denoising has been proven successful on sEMG signals acquired from the upper and lower limbs. Phinyomark et al. presented the idea to denoised the sEMG signal using the Wavelet Denoising algorithm [42]. Random noises like White Gaussian noise in sEMG signals are difficult to minimize by signal filtering; however, it can be effectively removed with the help of Wavelet Denoising. The white Gaussian noise *Y(n)* can be expressed as:

$$Y(n) = X(n) + H(n), \tag{1}$$

where *X(n)* is the original signal and *H(n)* is the noise signal.

The steps of the discrete wavelet transform based Wavelet Denoising are:

- Decompose the signal *Y(n)* by using the DWT;
- Select the threshold for each wavelet transform;
- Use inverse wavelet transform with threshold function to reconstruct the denoised signal.

When Wavelet Denoising is applied to signals, different wavelet coefficients are generated by passing the signal through High-Pass and Low-Pass filters. The approximation and detail coefficients are obtained after the decomposition of the signal by using the Wavelet Denoising technique. The number of coefficients depends on the level of decomposition. In this research, the Wavelet Denoising technique is used with *sym4* from the Symlet family to the first level of decomposition. After this, the thresholding can be performed. There are two traditional methods for thresholding the wavelet coefficient results: Hard and Soft thresholding [43]. Hard thresholding can keep only partial information of the original signal while soft thresholding has a constant deviation relative to the original signal. In this study, Universal thresholding is applied to the detailed coefficients. The universal thresholding selection rule [44] is defined as:

$$\lambda = \sigma\sqrt{2ln(N)}, \tag{2}$$

where σ = (MAD)/0.6745, with MAD referring to the Median Absolute Deviation of the wavelet coefficient and N is the signal length.

As an example, Figure 3 shows a raw sEMG signal and the corresponding denoised signal after applying the Wavelet Denoising technique.

3.2. Segmentation

The nature of a sEMG signal is stochastic, so segmented sEMG signal is more appropriate rather than the full sEMG signal. Different length of sEMG data affects the accuracy of the classification model. Two types of windowing techniques, called Adjacent and Overlapping, are usually used for sEMG signal segmentation [45]. Here, the overlapping windowing technique with a 256 ms time windowing and 25% of overlapping is used [46].

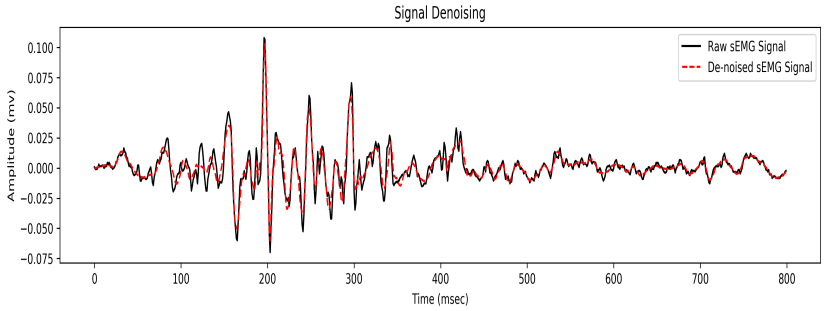

Figure 3: A raw sEMG Signal and the corresponding denoised sEMG signal obtained by Wavelet Decomposition.

3.3. Feature Extraction

In a raw sEMG signal, it has been seen that various noises and artifacts are present, which degrades its analysis accuracy because the required information remains as an amalgam in the raw sEMG signal. Therefore, to enhance the classification accuracy, the sEMG signal is denoised first, and then, features are extracted to be used as the input of a computational classifier. Three types of feature extraction techniques are available in the literature: time-domain (TD), frequency domain (FD) and time-frequency domain (TFD) feature. In this study, eleven time-domain features are used for knee abnormality identification from sEMG signals collected during walking [38].

- *Mean Absolute Value (MAV):* It is the average of N absolute values of a time series sample of sEMG signal (x_i) within a given time interval:

$$MAV = \frac{1}{N}\sum_{i=1}^{N}|x_i|\,. \tag{3}$$

- *Root Mean Square (RMS):* It is calculated by taking the square root of the arithmetic mean of the squared sample amplitude:

$$RMS = \sqrt{\frac{1}{N}\sum_{i=1}^{N}|x_i|^2}. \tag{4}$$

- *Zero Crossing (ZC):* It gives information about how many times the signal crosses the zero amplitude level:

$$ZC = \sum_{i=1}^{N-1} f\left(x_i \,.\, x_{i+1}\right), \tag{5}$$

where:

$$f(x) = \begin{cases} 1, & if, x < 0, \\ 0, & otherwise. \end{cases}$$

- *Slope Sign Change (SSC):* Similar to the zero crossing, SSC also gives information of frequency in terms of time domain features. Thus, it indicates how many times positive to negative or negative to positive slope transitions have taken place:

$$SSC = \sum_{i=2}^{N-1} f(x_i), \tag{6}$$

where:

$$f(x) = \begin{cases} 1, & if, (x_i > x_{i-1} \; and \; x_i > x_{i+1}) \;\; or \;\; (x_i < x_{i-1} \; and \; x_i < x_{i+1}), \\ 0, & otherwise. \end{cases}$$

- *Variance (VAR):* It gives information about the deviation of the signal from its mean value:

$$VAR = \frac{1}{N-1} \sum_{i=1}^{N} x_i^2. \tag{7}$$

- *Wilison Amplitude (WAMP):* It indicates the amount of stages resulting from amplitude change between two adjoining segments that exceeds a pre-defined threshold in the sEMG signal:

$$WAMP = \sum_{i=1}^{N-1} f(|(x_{i+1} - x_i)|), \tag{8}$$

where:

$$f(x) = \begin{cases} 1, & if, (x \geq Threshold), \\ 0, & otherwise. \end{cases}$$

- *Myopulse Percentage Rate (MYOP):* It is the average value of absolute values of the sEMG signal exceeding a pre-defined threshold:

$$MYOP = \frac{1}{N} \sum_{i=1}^{N} f(x_i), \tag{9}$$

where:

$$f(x) = \begin{cases} 1, & if, (x \geq Threshold), \\ 0, & otherwise. \end{cases}$$

- *Difference Absolute Standard Deviation Value (DASDV):* It is the standard deviation value of the wavelength:

$$DASDV = \sqrt{\frac{1}{N-1}\sum_{i=1}^{N-1}(x_{i+1}-x_i)^2}. \tag{10}$$

- *Average Amplitude Change (AAC):* It is the average cumulative length of the sEMG signal over the time segment:

$$AAC = \frac{1}{N}\sum_{i=1}^{N-1}|x_{i+1}-x_i|. \tag{11}$$

- *Skewness (Skew):* It is a measure related to the lack of symmetry or the asymmetry of the signal data:

$$Skew = \frac{E[(x-\mu)^3]}{\sigma^3}, \tag{12}$$

where σ is the standard deviation of the data, μ is the mean of the data, and E is the expected value estimator of the signal.

- *Kurtosis (Kurt):* It determines if the signal has a peak or is rather flat at its mean point:

$$Kurt = \frac{E[(x-\mu)^4]}{\sigma^4}. \tag{13}$$

Here, eleven time domain features for four different muscles, thus, 44 features were extracted. The length of the signal has been observed to be different for the two classes under classification; therefore, the number of samples of extracted features are different for the abnormal and healthy knee subjects.

3.4. Normalization

Normalization or Min-Max scaling is a re-scaling technique that shifts the range of the features to scale the range in between 0 (zero) to 1 (one) according to:

$$Y_{Fnew} = \frac{Y_{Fold} - Y_{Foldmin}}{Y_{Foldmax} - Y_{Foldmin}} \tag{14}$$

where Y_{Fnew} is the normalized EMG feature, Y_{Fold} is the actual EMG feature, $Y_{Foldmax}$ is the maximum value of the actual EMG feature, and $Y_{Foldmin}$ is the minimum value of the actual EMG feature.

3.5. Oversampling Techniques

As discussed previously, the length of the recorded sEMG data of abnormal knee subjects is different from the one of the normal subjects. An oversampling technique has then be used to balance the imbalanced class, i.e., to increase the number of samples of the minority class. On the one hand, if imbalanced data is used for training a classification model, then the data of majority categories would have dominated. On the other hand, if the data of minority classes are oversampled by duplicity, then an over fitting problem may occur due to repeated samples. Data level methods, algorithm level methods and hybrid methods are three approaches that have been used for handling the class imbalance problem.

Chawla et al. [47] proposed SMOTE for increasing the minority class. In the SMOTE approach, the minority class can be oversampled by creating synthetic cases in the feature space formed by the instance and its K-nearest neighbors as shown in Figure 4. The steps of the SMOTE oversampling technique are:

1. Choose K nearest neighbor from the minority samples ($X_i \in S_{min}$) according to the requirement of oversampling.
2. Randomly select a neighbor X_j ($X_j \in S_{min}$) from the K nearest neighbor.
3. A new synthetic sample is generated according to:
   $X_{new} = X_i + |X_j - X_i| * \delta$, where $\delta \in [0,1]$ is the random variable.

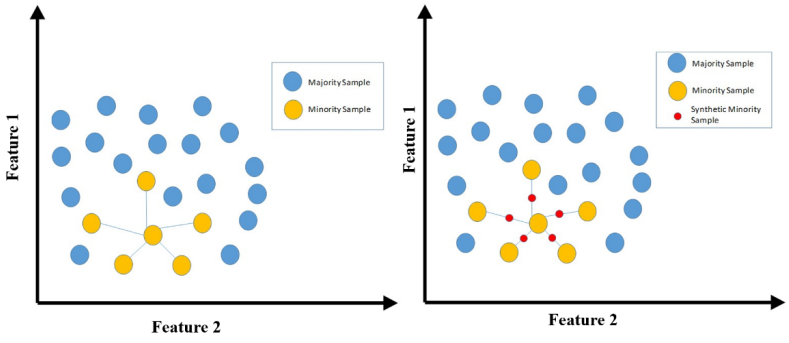

Figure 4: Illustration of the SMOTE oversampling approach.

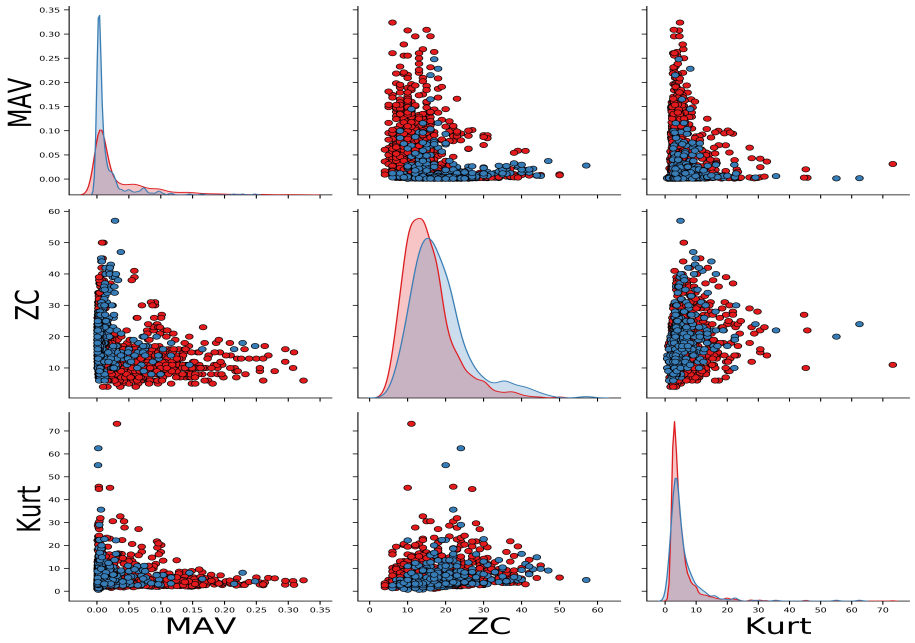

(a)

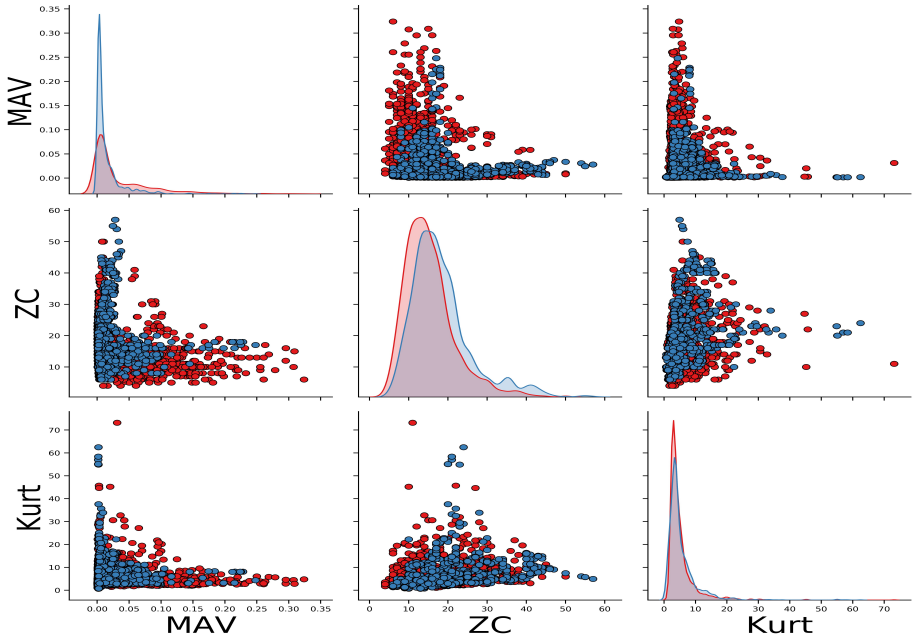

(b)

Figure 5: Pair plots for three extracted features: (a) without oversampling and (b) after the SMOTE oversampling.

Figure 5 shows the pair plots for three extracted features: Mean Absolute value, Zero Crossing and Kurtosis of the Rectus Femoris muscle for two cases, without oversampling and after the SMOTE oversampling. In these plots, blue circles indicate samples of healthy subjects and red circles indicate the samples of abnormal knee subjects. For all the three features, Figure 5(a) shows that the samples of abnormal knee subjects (red circles) are in higher number than those of the normal subjects (blue circles) and Figure 5(b) shows that the number of the samples of the minority class (blue circles) have increased after the SMOTE oversampling.

Another oversampling approach, Adaptive Synthetic oversampling (ADAYSN) has been proposed by Haibo et al. [48]. According to the data distribution, new data points of minority class can be generated using ADAYSN. In this technique, one can shift the decision boundary to focus on those difficult to learn samples and also reduce the learning bias that is introduced by the original imbalanced dataset. SVM SMOTE is also a variant of SMOTE oversampling where the borderline is defined based on the SVM hyper plane methodology[49].

3.6. Computational Classifiers

Once the features are extracted, and the oversampling is performed, computational techniques can be used to classify the data as from healthy subjects or abnormal knee subjects. In this study, Iterative Dichotomiser 3 (ID3), Classification and Regression Trees (CART), Bagging, Gradient Booster, Random Forest and Extra Tree based classifiers have been studied.

Iterative Dichotomiser 3 (ID3) is used to generate a decision tree [50]. It is a supervised learning algorithm for data classification that can be used for both categorical and numerical variables. It has no guarantee to give the optimal solution since it may converge upon local minima. Therefore, for splitting the input data, Greedy techniques are used to locally select the best attribute on each iteration. An over fitting problem may occur for the high depth of decision tree.

The steps of the Iterative Dichotomiser 3 classifier are:

- Step 1: Calculate the entropy of every attribute used in the data:

$$H(S) = -\sum_{y \varepsilon Y} \boldsymbol{p}(y) log_2 p(y), \tag{15}$$

  where S is the data where the entropy is calculated, Y is the set of classes in S, and $p(y)$ is the proportion of the elements in class y to the number of elements in S.

- Step 2: Split set S into subsets using the attribute where the information gain is maximum:

$$IG(S,A) = H(S) - H(S|A). \tag{16}$$

- Step 3: If the entropy is 0 (zero), then it is a leaf node and no further splitting is performed; however, if entropy is higher than 0 (zero), further splitting is needed and it should be performed as listed in step 2.

Classification and Regression Tree (CART) [51] is also a type of decision tree algorithm that can be used for classification and regression. It is similar to ID3 but the only difference is that ID3 uses information gain while CART uses the Gini index for splitting the data. Accordingly, the feature with a lower Gini index value is selected for splitting:

$$Gini = 1 - \sum_{i=1}^{n} (p_i)^2, \tag{17}$$

where p_i is the probability of a feature in a particular class.

Bagging Classifier [52] is an ensemble method that is used to build an accurate prediction model by combining the results of multiple machine learning algorithms. This classifier selects bootstrap (random) samples from the input data. It constructs n classification trees and calculates the prediction of individual classification trees, and then accumulates them to form the final prediction based on averaging or voting of the obtained individual outcomes. It is also called Bootstrap Algorithm as it can be used to reduce the high variance of a black-box estimator (e.g., a decision tree), by integrating randomization into its construction process and then making an ensemble out of it.

Gradient Boosting Classifier [53] is based on the idea of applying a weak learning algorithm repeatedly while improving the results from the previous ones sequentially

and finally build the classification as in a robust classifier. The Decision Tree is usually used as a weak learner. The performance is commonly measured by using the loss function at each iteration and optimized with the help of the Gradient Descent algorithm.

Random Forest Classifier [54] is an extension of the Decision Tree algorithm where bootstrap techniques are integrated. This classifier develops many classification trees rather than a single tree. It creates several bootstrap samples from the sample data and then develops a decision tree for each of the bootstrap samples. Random features are selected, and the features which give the best split are considered for splitting the node. The average number of votes from different trees are calculated, which provides the output of the overall prediction.

Extra Trees Classifier [55] is also called Extremely Randomized Decision Tree. It is also based on the Decision Tree algorithm and involves an ensemble decision tree like in the Random Forest algorithm. It differs from the Random Forest algorithm in two ways: (i) the training of each tree uses the entire training set instead of a random subset and (ii) the random splits are chosen instead of computing the locally best splits for each feature which makes this algorithm highly efficient.

Support Vector Machine Classifier [56] is a supervised machine learning algorithm where each data sample is plotted in a n-dimensional space and a hyper plane is constructed to separate the different classes optimally. This optimal decision surface can be constructed by maximizing the margin width between the nearest members of the classes.

Multilayer Perceptron Neural Network [57] is also a supervised learning algorithm. It is an artificial neural network that consists of three or more layers in a feed forward architecture with two layers dedicated to input and output while others are hidden layers. MLP uses a nonlinear activation function in the neurons and each layer is fully connected to the next layer.

3.7. Performance Measures

In this work, the problem under study is a binary classification problem which means either the subjects have knee abnormalities or not. In binary classification, the

classifier gives four possible outcomes, which are: True Positive (TP), i.e., correct positive prediction, True Negative (TN), i.e., correct negative prediction, False Positive (FP), i.e., incorrect positive prediction, and False Negative (FN), i.e., incorrect negative prediction. A confusion matrix may be built from these four outcomes, as illustrated in Table 1, and different performance measures may be calculated:

Table 1: Confusion Matrix.

		Predictive Class	
Actual Class		**Positive Class**	**Negative Class**
	Positive Class	True Positive (TP)	False Negative (FN)
	Negative Class	False Positive (FP)	True Negative (TN)

$$Accuracy = \frac{TP+TN}{TP+TN+FP+FN}, \tag{18}$$

$$Precision = \frac{TP}{TP+FP}, \tag{19}$$

$$Recall(Sensitivity) = \frac{TP}{TP+FN}, \tag{20}$$

$$Specificity = \frac{TN}{TN+FP}, \tag{21}$$

$$F1-Score = \frac{2*Recall*Precision}{Recall+Precision}. \tag{22}$$

For balanced data, accuracy can be considered as one of the evaluation metrics. In the case of imbalanced data, there is a need for other evaluation metrics such as sensitivity, specificity and F1-score, which have also been considered in this study [58].

4. Results

This section presents the results obtained using classifiers without and with oversampling techniques for the problem of knee abnormality detection from imbalance sEMG walking data. The obtained results seem to support the hypothesis that oversampling techniques improve the performance of the used classification model. The performance of the studied classifiers applied on original data (imbalanced data), and balanced data, obtained using oversampling techniques on the original data, was assessed using:

1. Selection of the optimal mother wavelet and decomposition level of the DWT denoising technique;
2. Performance analysis using the k-fold cross-validation technique;
3. Performance analysis according to a 95% confidence interval.

4.1. ***Selection of the optimal DWT denoising mother wavelet and level of decomposition***

The selection of the mother wavelet and decomposition level in wavelet transform denoising plays an important role. In this study, haar (db1), Daubechies (db4, db7, db9), symlet (sym2, sym4, sym5, sym7) and biorthogonal (bior1.1) have been used from the wavelet transform family with 1 to 10 levels of decomposition. here, the mother wavelet and decomposition level have been selected based on mean squared error (MSE), mean absolute error (MAE), signal to noise ratio (SNR), and peak signal to noise ratio (PSNR). These four metrics are commonly used to assess the performance of denoising methods. The MSE, MAE, SNR, and PSNR values were calculated from the sEMG signals of all 22 subjects using different levels of wavelet decomposition and then the mean value of these metrics was considered. A lower value of MSE and MAE and a higher value of SNR and PSNR indicate that the signal is accurately denoised. These four parameters were calculated for 9 mother wavelet functions with the fourth level of decomposition as shown in Table 2. It was also computed the same four metrics for the 1 to 10 levels of the wavelet decomposition with symlet4 mother wavelet as indicated in Table 3.

Table 2: Mean values of MSE, MAE, SNR and PSNR calculated from the sEMG signals of all 22 subjects using different mother wavelets (best values found are in bold).

Wavelet Function	MSE	MAE	SNR	PSNR
db1	0.00057	0.01081	7.94073	27.61071
db4	0.00042	0.00971	8.55542	28.22540
db7	0.00046	0.00994	8.30930	27.97928
db9	0.00048	0.01005	8.16712	27.83709
sym2	0.00045	0.00998	8.43299	28.10296
sym4	**0.00039**	**0.00941**	**8.82642**	**28.49640**
sym 5	0.00040	0.00947	8.77723	28.44721
sym7	0.00040	0.00953	8.71923	28.38921
bior1.1	0.00057	0.01081	7.94073	27.61071

4.2. Performance analysis using k-fold cross validation

K-fold cross-validation is a method of re-sampling using constrained data to validate the performance of machine learning models. In this approach, the input data is randomly split into k groups of equal size. Then, the model is trained using $k - 1$ groups of data and validated with the k^{th} group. Here, the performance of the studied classification models was assessed using 10-fold cross-validation [59] in four sEMG walking knee datasets:

1. The original data (imbalanced data);
2. The balanced data obtained by SMOTE oversampling;
3. The balanced data obtained by ADASYN oversampling;
4. The balanced data obtained by SVM SMOTE oversampling.

The obtained results are presented in Table 4.

4.3. Performance analysis according to a 95% confidence interval

For testing the statistical significance, an experiment was conducted for 100 randomized tests for measurement of accuracy, sensitivity, specificity and F1-score perfor-mance metrics were calculated according to a 95% confidence interval. The obtained results are summarized in Table 5.

Table 3: Mean values of MSE, MAE, SNR and PSNR calculated from the sEMG signals of all 22 subjects using different levels of wavelet decomposition (best values found are in bold).

Decomposition Level	MSE	MAE	SNR	PSNR
D1	**0.00001**	**0.00142**	**24.31335**	**43.98333**
D2	0.00005	0.00318	17.68627	37.35625
D3	0.00015	0.00592	12.42797	32.09795
D4	0.00039	0.00941	8.82642	28.49640
D5	0.00100	0.01368	6.65022	26.32019
D6	0.00157	0.01650	5.63505	25.30503
D7	0.00170	0.01703	5.42477	25.09475
D8	0.00171	0.01707	5.40338	25.07336
D9	0.00171	0.01706	5.40112	25.07110
D10	0.00172	0.01709	5.39753	25.06750

5. Discussion

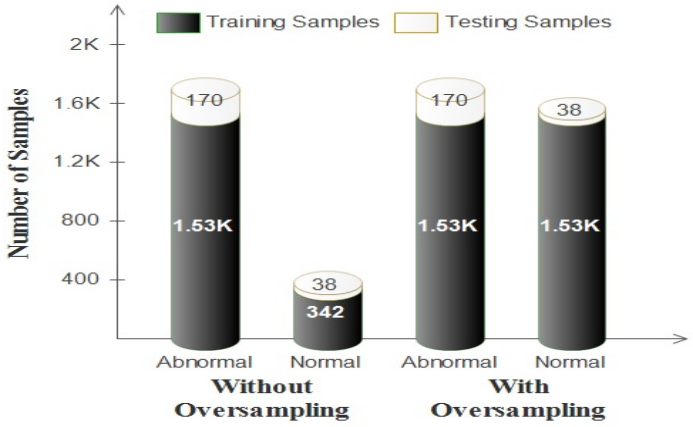

Figure 6: Number of samples used in training and testing the classifiers with and without data oversampling.

Figure 6 shows the number of samples used in training and testing the classifiers with and without oversampling. In the case of Without oversampling, the classification models were trained with 342 and 1533 samples of the extracted features from healthy and abnormal knee subjects, respectively, and tested with 38 and 170 samples. On the other hand, with oversampling, the number of the training samples of normal subjects

Table 4: Performance obtained by each classifier when applied on the original data and on the oversampled data (best values found in bold.)

Oversampling	Classifier	Accuracy		Sensitivity		Specificity		F-Score	
Original	ID3	83.2	1.5	0.935	0.016	0.379	0.059	0.536	0.059
	CART	82.8	1.5	0.951	0.03	0.276	0.137	0.405	0.194
	Bagging	89.5	1.5	0.979	0.011	0.518	0.067	0.675	0.058
	Gradient Boosting	89.4	2.2	0.972	0.017	0.545	0.086	0.694	0.071
	Random Forest	90.9	1.1	0.981	0.01	0.587	0.047	0.733	0.037
	SVM	86.5	1.5	989	0.012	0.308	0.053	0.467	0.06
	MLP	84.9	2.2	0.965	0.021	0.329	0.141	0.471	0.181
	Extra Tree	**91.9**	1.1	0.984	0.008	0.629	0.065	**0.765**	0.048
SMOTE	ID3	76.2	3.8	0.787	0.56	0.647	0.123	0.700	0.07
	CART	75.6	4.3	0.771	0.061	0.687	0.109	0.718	0.052
	Bagging	89.2	1.8	0.937	0.016	0.689	0.067	0.793	0.045
	Gradient Boosting	87.5	1.9	0.893	0.022	0.792	0.066	0.838	0.036
	Random Forest	90.7	2	0.937	0.02	0.776	0.063	0.848	0.038
	SVM	81.4	2	0.812	0.024	0.824	0.065	0.816	0.03
	MLP	85.5	2.8	0.878	0.035	0.75	0.063	0.807	0.036
	Extra Tree	**93.1**	1.1	0.969	0.01	0.763	0.054	**0.853**	0.033
ADASYN	ID3	63.5	6.2	0.604	0.089	0.774	0.088	0.668	0.047
	CART	62.8	6.4	0.596	0.094	0.771	0.109	0.659	0.046
	Bagging	87.8	2.4	919	0.018	0.695	0.09	0.788	0.06
	Gradient Boosting	86.4	1.5	0.878	0.019	0.8	0.054	0.836	0.027
	Random Forest	90.3	2.4	0.93	0.023	0.782	0.063	**0.847**	0.03
	SVM	78.1	2.7	0.758	0.034	0.887	0.054	0.816	0.027
	MLP	83.2	3.1	0.835	0.033	0.821	0.085	0.825	0.047
	Extra Tree	**92.2**	1.8	0.96	0.017	0.753	0.067	0.842	0.043
SVM SMOTE	ID3	71.7	4.6	0.713	0.063	0.734	0.08	0.718	0.04
	CART	73	5.3	0.726	73	0.75	0.102	0.73	0.049
	Bagging	90.2	2.4	0.937	0.024	0.745	0.084	0.827	0.053
	Gradient Boosting	88.1	2.2	0.897	0.022	0.808	0.086	0.847	0.048
	Random Forest	91	2.4	0.941	0.021	0.774	0.083	0.847	0.053
	SVM	81.8	2.3	0.824	0.03	0.789	0.078	0.803	0.04
	MLP	85.3	2.2	0.873	0.027	0.766	0.078	0.813	0.044
	Extra Tree	**93.2**	1.8	**0.97**	0.014	0.761	0.07	**0.851**	0.044

Table 5: Performance obtained by each classifier when applied on the original data and on the balanced data obtained by oversampling according to a 95% confidence Interval (best values found in bold).

Oversampling	Classifier	Accuracy		Sensitivity		Specificity		F-Score	
		Lower	Upper	Lower	Upper	Lower	Upper	Lower	Upper
Original	ID3	82.93	83.04	0.9319	0.933	0.366	0.3732	0.5198	0.5276
	CART	82.78	82.92	0.9499	0.9522	0.2718	0.2855	0.3955	0.4141
	Bagging	89.54	89.68	0.9762	0.9773	0.5317	0.5379	0.6843	0.6896
	Gradient Boosting	89.48	89.6	0.9751	0.976	0.5339	0.5391	0.6863	0.6907
	Random Forest	90.87	91	0.9807	0.9816	0.5845	0.5903	0.7293	0.734
	SVM	**86.46**	**86.52**	**0.9891**	**0.9894**	0.3053	0.3081	0.4623	0.4658
	MLP	85.41	85.65	0.9647	0.9668	**0.3516**	**0.369**	**0.4968**	**0.5177**
	Extra Tree	**91.63**	91.75	0.9833	0.9841	0.615	0.6207	**0.7539**	0.7583
SMOTE	ID3	73.36	73.82	0.7461	0.7525	0.6721	0.6795	0.7029	0.7071
	CART	72.44	72.99	0.7348	0.7426	0.6715	0.6796	0.6964	0.7002
	Bagging	88.89	89.06	0.9358	0.9374	0.6768	0.6826	0.7829	0.7869
	Gradient Boosting	87.12	87.27	0.8944	0.8958	0.7662	0.7705	0.8237	0.8263
	Random Forest	90.78	90.91	0.9392	0.9406	0.765	0.7696	0.8416	0.8445
	SVM	81.46	81.59	0.8147	0.8161	0.8128	0.8159	0.8123	0.8141
	MLP	82.05	82.35	0.8289	0.8328	0.7789	0.7853	0.8013	0.8049
	Extra Tree	**92.5**	92.64	0.9661	0.9671	0.7399	0.7454	**0.836**	0.8397
ADASYN	ID3	63.64	64.28	0.6033	0.6121	0.7788	0.787	0.6747	0.6794
	CART	63.94	64.6	**0.609**	**0.6183**	0.7684	0.7777	0.6742	0.6788
	Bagging	88.26	88.44	0.9269	0.9286	0.6823	0.6867	0.7834	0.7879
	Gradient Boosting	**85.7**	**86.89**	0.8744	0.8763	0.7773	0.7825	0.8215	0.8247
	Random Forest	90.3	90.45	0.9307	0.9323	0.777	0.7818	**0.8456**	0.8486
	SVM	77.4	77.52	0.7506	0.752	**0.8782**	**0.8807**	**0.8085**	**0.8098**
	MLP	78.28	78.8	0.7747	0.7802	0.8206	0.8268	0.7947	0.7992
	Extra Tree	**92.43**	92.56	0.9614	0.9627	0.7562	0.761	0.845	0.8479
SVM SMOTE	ID3	73.53	73.91	0.7412	0.7469	0.7025	0.7106	0.7162	0.7197
	CART	72.95	73.43	0.7306	0.738	0.7165	0.726	0.7176	0.7215
	Bagging	89.41	89.56	0.935	0.9365	0.7086	0.7147	0.8038	0.8078
	Gradient Boosting	87.36	87.5	0.8939	0.8954	0.7809	0.7856	0.8321	0.8349
	Random Forest	91	91.14	0.9384	0.9398	0.7812	0.7864	0.8513	0.8543
	SVM	82.07	82.28	0.8253	0.8284	0.7969	0.8016	0.8095	0.8113
	MLP	82.88	83.19	0.8419	0.846	0.7657	0.7728	0.8001	0.8038
	Extra Tree	**92.5**	92.62	**0.9653**	0.9663	0.7425	0.748	**0.8375**	0.8411

was increased from 342 to 1533, and then the classification models were trained with 1533 samples of the extracted features from both healthy and knee abnormal subjects, and the testing was performed using the same number of samples of the without over-sampling case.

Table 2 presents a comparative analysis in terms of MSE, MAE, SNR and PSNR values that were obtained using different mother wavelet functions for denoising the input signal. The results show that symlet4 led to the lowest MAE and MSE values along with the highest SNR and PSNR values. Therefore, symlet4 was employed as the mother wavelet function. Table 3 presents the results as to MSE, MAE, SNR and PSNR metrics obtained using different wavelet decomposition levels to denoising the input signal. The results show that the first level of decomposition led to the lowest MAE and MSE values along with the highest SNR and PSNR values. Therefore, the decomposition level 1 (D1) was considered.

Table 4 allows the performance comparison of the different classifiers when used in combination with different oversampling methods. The results support the hypothesis that the oversampling improves all performance metrics. The Extra Tree classifier obtained the highest accuracy and F1-score, and was followed by SVM, MLP, random forest, gradient boosting, bagging, CART and ID3.

In the case of the original data without oversampling, i.e., the imbalanced data, the Extra Tree classifier obtained an accuracy of 91.9% while for the MLP, SVM, Random Forest, Gradient Boosting, Bagging, CART and ID3 classifiers, it was of 84.9%, 86.5%, 90.9%, 89.4% , 89.5%, 82.8%, and 83.2%, respectively, as indicated in Table 4. Similarly, F1-score was of 76.5%, 47.1%, 46.7%, 73.3%, 69.4%, 67.5%, 40.5% and 53.6% for the Extra Tree, MLP, SVM, Random Forest, Gradient Boosting, Bagging, CART and ID3 classifiers, respectively. In this case, the accuracy and sensitivity values were observed to be good, but the values obtained for the other performance metrics, mainly for F1-score and specificity, were not so interesting.

After the use of the different oversampling techniques, it was found out that the classification accuracy could not be improved, but the other performance measures, mainly F1-Score and sensitivity, had better values than the ones obtained from the original data. In the case of oversampling by SMOTE, the accuracies were of 93.1%,

85.5%, 81.4%, 90.7%, 87.5%, 89.2%, 75.6% and 76.2%, and as to F-score were of 85.3%, 80.7%, 81.6%, 84.3%, 83.8%, 79.3%, 71.8% and70.0% for the extra tree, SVM, MLP, random forest, gradient boosting, bagging, CART and ID3 classifiers, respectively, as indicated in Table 4.

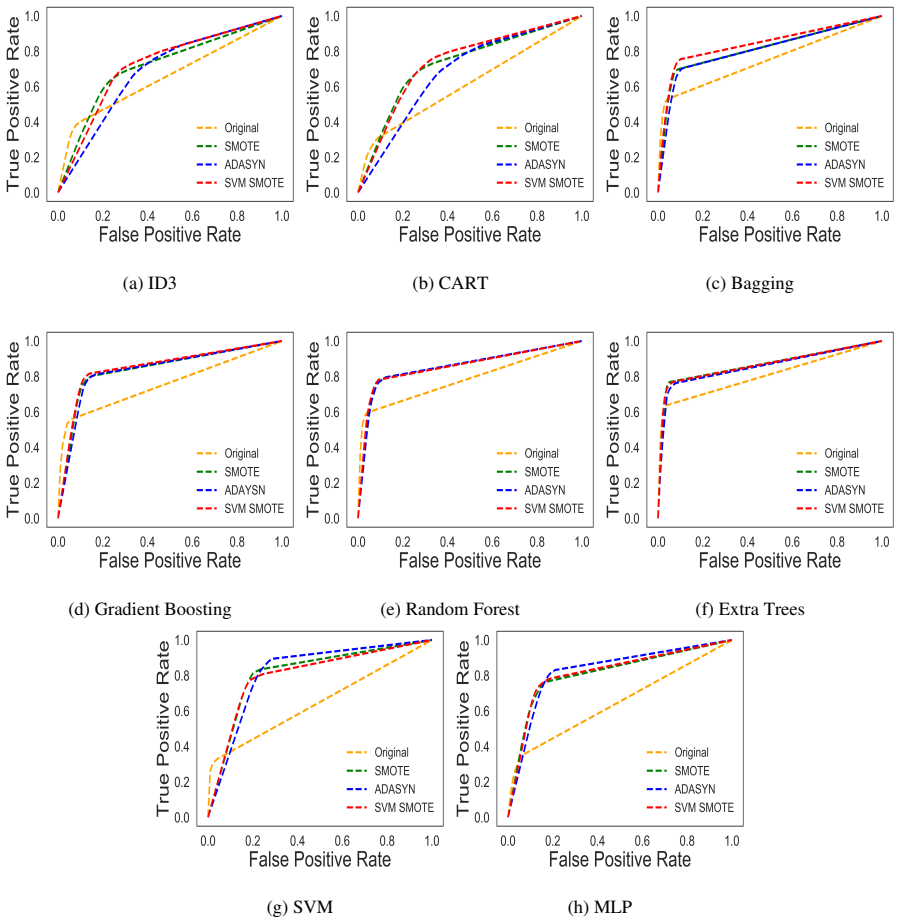

Figure 7: ROC curve of classifier with and without oversampling techniques

A receiver operating characteristic (ROC) curve is a tool commonly used to analyze the performance of classification models, mainly in two class classification problems. It is a graphical representation between the true positive rate (sensitivity) and false positive rate (1-specificity) [60]. Figure 7 shows the ROC curve obtained for the studied classifiers when applied to the original data and oversampled data. For all classifiers,

the ROC curve built as to the oversampled data is far better than the one built from the as to the original data.

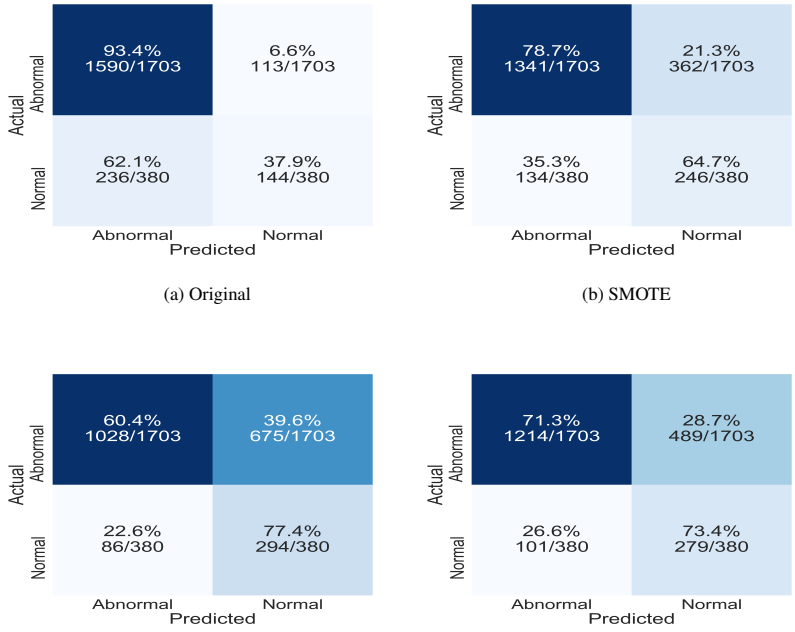

(a) Original (b) SMOTE

(c) ADASYN (d) SVM SMOTE

Figure 8: Confusion Matrix of the ID3 classifier with and without oversampling.

Figures 8 shows the confusion matrices obtained for the ID3 and Extra Tree classifiers without data oversampling. The confusion matrix allows conceptualizing the performance of a classification algorithm in a tabular form. It contains information about the true and predicted labels evaluated by a model. In Figure 8(a), it can be seen that 62.1% of the samples of normal subjects were wrongly predicted as of abnormal subjects and 93.4% of the samples of abnormal subjects were correctly predicted as of abnormal subjects. Figures 8 (b-d) show the confusion matrix of ID3 classifier obtained with different oversampling methods. From these confusion matrices, it is concluded that the used classification models were biased towards the majority class (abnormal subjects) with the original dataset but when minority class data is increased by using oversampling techniques then the classification models were not found as biased on a

single class.

Data distribution can be analyzed with the help of box plots. Figure 9 shows the box plot distributions for f-score with oversampling techniques of all studied classifiers according to the 10-fold cross-validation technique. For all the classifiers, the f-score obtained with oversampling was found to be far better than the one obtained without oversampling.

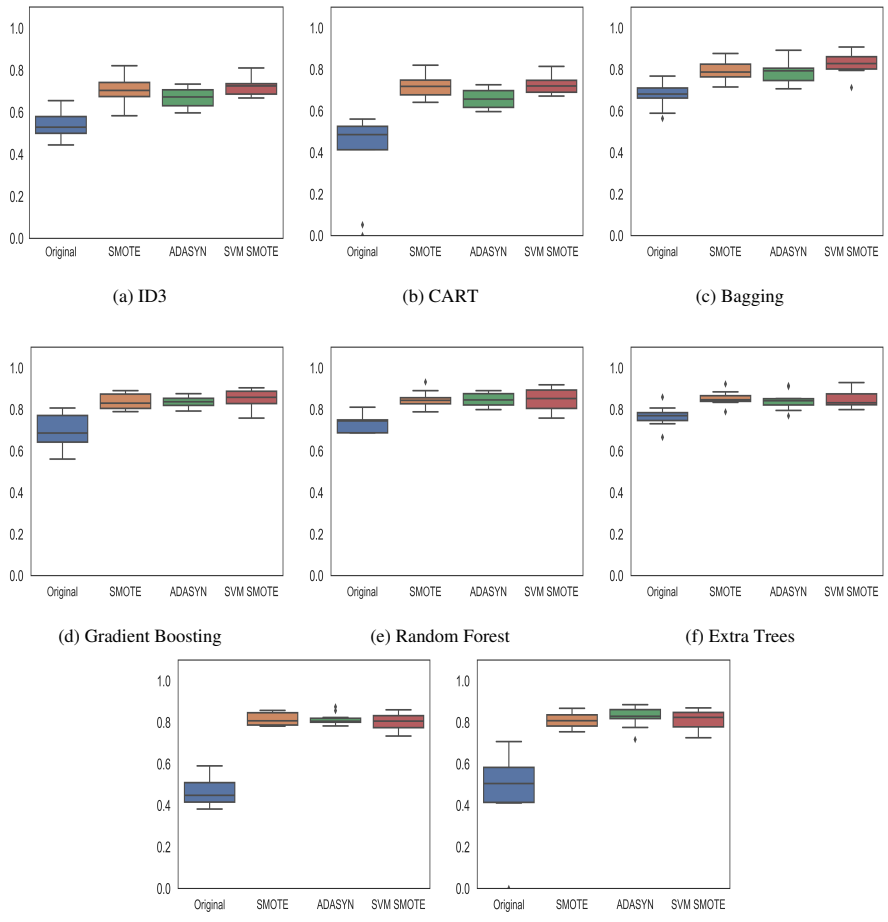

(a) ID3 (b) CART (c) Bagging

(d) Gradient Boosting (e) Random Forest (f) Extra Trees

(g) SVM (h) MLP

Figure 9: Box plot for each classifier with applied oversampling techniques according to 10-fold cross validation.

Table 5 shows the performance metrics obtained for each studied classifier accord-

ing to a 95% confidence interval for 100 randomized tests. From the presented results, it may be observed that the range of values for all the metrics obtained for the different classifiers are narrow, for without and with oversampling. This allows for the conclusion that their respective distributions are not heterogeneous.

Furthermore, no significant difference was found between the performance metrics of the different oversampling techniques that have been implemented. However, if the results are compared in terms of with and without oversampling, then one can conclude that the oversampling can lead to promising knee abnormality detection even from imbalanced sEMG data, independent of the classification model that is used.

6. Conclusion

Imbalanced data is a major problem in the classification of medical data, which may arise either due to the high differences in the number of healthy and unhealthy subjects or due to the length of the collected data be different for normal and abnor-mal subjects. In this work, the input raw sEMG signal was denoised by the Wavelet Denoising technique. After removing the noise, the sEMG signal was segmented and eleven-time domain features were extracted. After obtaining the features, the number of minority class samples was increased by using oversampling techniques, and then the performance of different classifiers on the imbalanced data and the oversampled, i.e., balanced, data was assessed. The obtained results suggest that oversampling techniques improve the performance of the classifiers in cases of imbalanced data. For that, four performance metrics (Accuracy, Sensitivity, Selectivity, and F1-Score) were used to assess the classification accuracy of the sEMG data acquired from abnormal knee and healthy subjects during walking in terms of knee abnormality detection during walking.

In this study, one offline sEMG dataset was used to test the proposed approach. In the future, the approach can be validated using a large dataset acquired in real-time in a clinical scenario, which can validate its clinical use. Further, the classification can be performed without handcrafted feature extraction, and one may also try to reduce the extracted features space by using feature reduction techniques, which may decrease the

computational time and improve the classification accuracy.

Compliance with ethical standards

Conflict of interest Authors declare no conflict of interest.

Ethical approval This article does not contain any study with human participants per-formed by any of the authors.

References

[1] A. Foundation, Arthritis by the numbers (2017).

[2] J. L. Baldwin, The anatomy of the medial patellofemoral ligament, The American journal of sports medicine 37 (12) (2009) 2355–2361.

[3] A. Praemer, Musculoskeletal conditions in the united states, Am Acad Orthop Surg 22 (1976) 1–199.

[4] J. Hemavathi, T. S. Kumar, R. K. Prasad, Knee vibratography: Arthritis diagnosis through non-invasive cloud based artificial intelligence, in: 2017 2nd International Conference on Computational Systems and Information Technology for Sustainable Solution (CSITSS), IEEE, 2017, pp. 1–6.

[5] J. Bedson, K. Jordan, P. Croft, How do gps use x rays to manage chronic knee pain in the elderly? a case study, Annals of the rheumatic diseases 62 (5) (2003) 450–454.

[6] S. Kubakaddi, K. Ravikumar, D. Harini, Measurement of cartilage thickness for early detection of knee osteoarthritis (koa), in: 2013 IEEE Point-of-Care Healthcare Technologies (PHT), IEEE, 2013, pp. 208–211.

[7] Prakash, Chandra and Kumar, Rajesh and Mittal, Namita, Recent developments in human gait research: parameters, approaches, applications, machine learning techniques, datasets and challenges, Artificial Intelligence Review 49 (1) (2018) 1–40.

[8] B.-S. Yang, S.-T. Liao, Fall detecting using inertial and electromyographic sensors, in: Proceedings of the 36th Annual Meeting of the American Society of Biomechanics, Gainsville, FL, USA, 2012, pp. 15–18.

[9] J. Cheng, X. Chen, M. Shen, A framework for daily activity monitoring and fall detection based on surface electromyography and accelerometer signals, IEEE journal of biomedical and health informatics 17 (1) (2012) 38–45.

[10] R. Merletti, C. J. De Luca, New techniques in surface electromyography (1989).

[11] Kanoga, Suguru and Kanemura, Atsunori and Asoh, Hideki, Are armband semg devices dense enough for long-term use?—sensor placement shifts cause significant reduction in recognition accuracy, Biomedical Signal Processing and Control 60 (2020) 101981.

[12] J. Yin, Q. Yang, J. J. Pan, Sensor-based abnormal human-activity detection, IEEE Transactions on Knowledge and Data Engineering 20 (8) (2008) 1082–1090.

[13] S. K. Au, P. Bonato, H. Herr, An emg-position controlled system for an active ankle-foot prosthesis: an initial experimental study, in: 9th International Conference on Rehabilitation Robotics, 2005. ICORR 2005., IEEE, 2005, pp. 375–379.

[14] C. S. Pattichis, C. N. Schizas, Genetics-based machine learning for the assessment of certain neuromuscular disorders, IEEE Transactions on Neural Networks 7 (2) (1996) 427–439.

[15] L. Burkow-Heikkinen, Non-invasive physiological monitoring of exercise and fit-ness, Neurological Research 33 (1) (2011) 3–17.

[16] P. K. Shukla, A. Vijayvargiya, R. Kumar, et al., Human activity recognition using accelerometer and gyroscope data from smartphones, in: 2020 International Conference on Emerging Trends in Communication, Control and Computing (ICONC3), IEEE, 2020, pp. 1–6.

[17] Hudgins, Bernard and Parker, Philip and Scott, Robert N, A new strategy for multifunction myoelectric control, IEEE Transactions on Biomedical Engineering 40 (1) (1993) 82–94.

[18] Huang, Yanjiang and Chen, Kaibin and Zhang, Xianmin and Wang, Kai and Ota, Jun, Joint torque estimation for the human arm from semg using backpropagation neural networks and autoencoders, Biomedical Signal Processing and Control 62 (2020) 102051.

[19] Da Silva, USLG and Villagra, HA and Oliva, LL and Marconi, NF, Emg activity of upper limb on spinal cord injury individuals during whole-body vibration, Physiology International (Acta Physiologica Hungarica) 103 (3) (2016) 361–367.

[20] S. Sudarsan, I. Student Member, E. C. Sekaran, Design and development of emg controlled prosthetics limb, Procedia engineering 38 (2012) 3547–3551.

[21] T. Tuncer, S. Dogan, A. Subasi, Surface emg signal classification using ternary pattern and discrete wavelet transform based feature extraction for hand movement recognition, Biomedical Signal Processing and Control 58 (2020) 101872.

[22] S. Cai, Y. Chen, S. Huang, Y. Wu, H. Zheng, X. Li, L. Xie, Svm-based classification of semg signals for upper-limb self-rehabilitation training, Frontiers in Neurorobotics 13 (2019) 31.

[23] Krawczyk, Bartosz, Learning from imbalanced data: open challenges and future directions, Progress in Artificial Intelligence 5 (4) (2016) 221–232.

[24] A. Rainoldi, G. Melchiorri, I. Caruso, A method for positioning electrodes during surface emg recordings in lower limb muscles, Journal of neuroscience methods 134 (1) (2004) 37–43.

[25] G. S. Murley, H. B. Menz, K. B. Landorf, A. R. Bird, Reliability of lower limb electromyography during overground walking: a comparison of maximal-and sub-maximal normalisation techniques, Journal of biomechanics 43 (4) (2010) 749–756.

[26] H. Huang, F. Zhang, L. J. Hargrove, Z. Dou, D. R. Rogers, K. B. Engle-hart, Continuous locomotion-mode identification for prosthetic legs based on neuromuscular–mechanical fusion, IEEE Transactions on Biomedical Engineering 58 (10) (2011) 2867–2875.

[27] S. Mulroy, J. Gronley, W. Weiss, C. Newsam, J. Perry, Use of cluster analysis for gait pattern classification of patients in the early and late recovery phases following stroke, Gait & posture 18 (1) (2003) 114–125.

[28] J. Chen, X. Zhang, Y. Cheng, N. Xi, Surface emg based continuous estimation of human lower limb joint angles by using deep belief networks, Biomedical Signal Processing and Control 40 (2018) 335–342.

[29] P. Bonato, M. Heng, J. Gonzalez-Cueto, A. Leardini, J. O'Connor, S. H. Roy, Emg-based measures of fatigue during a repetitive squat exercise, IEEE engineering in medicine and biology magazine 20 (6) (2001) 133–143.

[30] R. Swaroop, M. Kaur, P. Suresh, P. K. Sadhu, Classification of myopathy and neuropathy emg signals using neural network, in: 2017 International Conference on Circuit, Power and Computing Technologies (ICCPCT), IEEE, 2017, pp. 1–5.

[31] P. Kugler, C. Jaremenko, J. Schlachetzki, J. Winkler, J. Klucken, B. Eskofier, Automatic recognition of parkinson's disease using surface electromyography during standardized gait tests, in: 2013 35th Annual International Conference of the IEEE Engineering in Medicine and Biology Society (EMBC), IEEE, 2013, pp. 5781–5784.

[32] Morbidoni, Christian and Cucchiarelli, Alessandro and Fioretti, Sandro and Di Nardo, Francesco, A deep learning approach to emg-based classification of gait phases during level ground walking, Electronics 8 (8) (2019) 894.

[33] Takhar, Gourav and Prakash, Chandra and Mittal, Namita and Kumar, Rajesh, Vision-based gender recognition using hybrid background subtraction technique, in: International Conference on Next Generation Computing Technologies, Springer, 2017, pp. 651–662.

[34] K. N. Rajesh, R. Dhuli, Classification of imbalanced ecg beats using re-sampling techniques and adaboost ensemble classifier, Biomedical Signal Processing and Control 41 (2018) 242–254.

[35] J. Nahar, T. Imam, K. S. Tickle, A. S. Ali, Y.-P. P. Chen, Computational intelligence for microarray data and biomedical image analysis for the early diagnosis of breast cancer, Expert Systems with Applications 39 (16) (2012) 12371–12377.

[36] L. Taft, R. S. Evans, C. Shyu, M. Egger, N. Chawla, J. Mitchell, S. N. Thornton, B. Bray, M. Varner, Countering imbalanced datasets to improve adverse drug event predictive models in labor and delivery, Journal of biomedical informatics 42 (2) (2009) 356–364.

[37] O. Sanchez, J. Sotelo, M. Gonzales, G. Hernandez, Emg dataset in lower limb data set, UCI machine learning repository (2014) 2014–02.

[38] R. Chowdhury, M. Reaz, M. Ali, A. Bakar, K. Chellappan, T. Chang, Surface electromyography signal processing and classification techniques, Sensors 13 (9) (2013) 12431–12466.

[39] C.-F. Jiang, S.-L. Kuo, A comparative study of wavelet denoising of surface electromyographic signals, in: 2007 29th Annual International Conference of the IEEE Engineering in Medicine and Biology Society, IEEE, 2007, pp. 1868–1871.

[40] A. O. Andrade, S. Nasuto, P. Kyberd, C. M. Sweeney-Reed, F. Van Kanijn, Emg signal filtering based on empirical mode decomposition, Biomedical Signal Processing and Control 1 (1) (2006) 44–55.

[41] Altan, Gokhan and Kutlu, Yakup and Allahverdi, Novruz, Deep belief networks based brain activity classification using eeg from slow cortical potentials in stroke, International Journal of Applied Mathematics, Electronics and Computers 4 (2016) 205–210.

[42] Phinyomark, Angkoon and Phukpattaranont, Pornchai and Limsakul, Chusak, Wavelet-based denoising algorithm for robust emg pattern recognition, Fluctuation and Noise Letters 10 (02) (2011) 157–167.

[43] A. Graps, An introduction to wavelets, IEEE computational science and engineering 2 (2) (1995) 50–61.

[44] C. He, J. Xing, J. Li, Q. Yang, R. Wang, A new wavelet threshold determination method considering interscale correlation in signal denoising, Mathematical Problems in Engineering 2015 (2015).

[45] O. Banos, J.-M. Galvez, M. Damas, H. Pomares, I. Rojas, Window size impact in human activity recognition, Sensors 14 (4) (2014) 6474–6499.

[46] G. R. Naik, S. E. Selvan, S. P. Arjunan, A. Acharyya, D. K. Kumar, A. Ramanujam, H. T. Nguyen, An ica-ebm-based semg classifier for recognizing lower limb movements in individuals with and without knee pathology, IEEE Transactions on Neural Systems and Rehabilitation Engineering 26 (3) (2018) 675–686.

[47] N. V. Chawla, K. W. Bowyer, L. O. Hall, W. P. Kegelmeyer, Smote: synthetic minority over-sampling technique, Journal of artificial intelligence research 16 (2002) 321–357.

[48] He, H and Bai, Y and Garcia, E and Li, S ADASYN, Adaptive synthetic sampling approach for imbalanced learning. ieee international joint conference on neural networks, 2008 (ieee world congress on computational intelligence) (2008).

[49] Q. Wang, Z. Luo, J. Huang, Y. Feng, Z. Liu, A novel ensemble method for imbalanced data learning: bagging of extrapolation-smote svm, Computational intelligence and neuroscience 2017 (2017).

[50] Quinlan, J. Ross, Induction of decision trees, Machine learning 1 (1) (1986) 81–106.

[51] D. H. Moore, Classification and regression trees, by leo breiman, jerome h. friedman, richard a. olshen, and charles j. stone. brooks/cole publishing, monterey, 1984, 358 pages, Cytometry: The Journal of the International Society for Analytical Cytology 8 (5) (1987) 534–535.

[52] L. Breiman, Bagging predictors, Machine learning 24 (2) (1996) 123–140.

[53] L. Mason, J. Baxter, P. L. Bartlett, M. R. Frean, Boosting algorithms as gradient descent, in: Advances in neural information processing systems, 2000, pp. 512–518.

[54] L. Breiman, Random forests, Machine learning 45 (1) (2001) 5–32.

[55] P. Geurts, D. Ernst, L. Wehenkel, Extremely randomized trees, Machine learning 63 (1) (2006) 3–42.

[56] Xuegong, Zhang, Introduction to statistical learning theory and support vector machines, Acta Automatica Sinica 26 (1) (2000) 32–42.

[57] X. Zhai, A. A. S. Ali, A. Amira, F. Bensaali, Mlp neural network based gas classification system on zynq soc, IEEE Access 4 (2016) 8138–8146.

[58] G. Altan, Y. Kutlu, A. Ö. Pekmezci, S. Nural, Deep learning with 3d-second order difference plot on respiratory sounds, Biomedical Signal Processing and Control 45 (2018) 58–69.

[59] Kohavi, Ron and others, A study of cross-validation and bootstrap for accuracy estimation and model selection, in: Ijcai, Vol. 14, Montreal, Canada, 1995, pp. 1137–1145.

[60] N. Nazmi, A. Rahman, M. Azizi, S.-I. Yamamoto, S. A. Ahmad, H. Zamzuri, S. A. Mazlan, A review of classification techniques of emg signals during isotonic and isometric contractions, Sensors 16 (8) (2016) 1304.